

# Fatty Acid Binding Protein 5 Modulates Docosahexaenoic Acid-Induced Recovery in Rats Undergoing Spinal Cord Injury

Johnny D. Figueroa,<sup>1</sup> Miguel Serrano-Illan,<sup>1</sup> Jenniffer Licero,<sup>1</sup> Kathia Cordero,<sup>1</sup>  
Jorge D. Miranda,<sup>2</sup> and Marino De Leon<sup>1</sup>

## Abstract

Omega-3 polyunsaturated fatty acids (n-3 PUFAs) promote functional recovery in rats undergoing spinal cord injury (SCI). However, the precise molecular mechanism coupling n-3 PUFAs to neurorestorative responses is not well understood. The aim of the present study was to determine the spatiotemporal expression of fatty acid binding protein 5 (FABP5) after contusive SCI and to investigate whether this protein plays a role in n-3 PUFA-mediated functional recovery post-SCI. We found that SCI resulted in a robust spinal cord up-regulation in FABP5 mRNA levels ( $556 \pm 187\%$ ) and protein expression ( $518 \pm 195\%$ ), when compared to sham-operated rats, at 7 days post-injury (dpi). This upregulation coincided with significant alterations in the metabolism of fatty acids in the injured spinal cord, as revealed by metabolomics-based lipid analyses. In particular, we found increased levels of the n-3 series PUFAs, particularly docosahexaenoic acid (DHA; 22:6 n-3) and eicosapentaenoic acid (EPA; 20:5 n-3) at 7 dpi. Animals consuming a diet rich in DHA and EPA exhibited a significant upregulation in FABP5 mRNA levels at 7 dpi. Immunofluorescence showed low basal FABP5 immunoreactivity in spinal cord ventral gray matter NeuN<sup>+</sup> neurons of sham-operated rats. SCI resulted in a robust induction of FABP5 in glial (GFAP<sup>+</sup>, APC<sup>+</sup>, and NG2<sup>+</sup>) and precursor cells (DCX<sup>+</sup>, nestin<sup>+</sup>). We found that continuous intrathecal administration of FABP5 silencing with small interfering RNA (2  $\mu$ g) impaired spontaneous open-field locomotion post-SCI. Further, FABP5 siRNA administration hindered the beneficial effects of DHA to ameliorate functional recovery at 7 dpi. Altogether, our findings suggest that FABP5 may be an important player in the promotion of cellular uptake, transport, and/or metabolism of DHA post-SCI. Given the beneficial roles of n-3 PUFAs in ameliorating functional recovery, we propose that FABP5 is an important contributor to basic repair mechanisms in the injured spinal cord.

**Key words:** DHA; locomotion; n-3 fatty acids; repair; spinal cord injury

## Introduction

**S**PINAL CORD INJURY (SCI) elicits a highly debilitating pathology leading to significant neurological dysfunction. Initial trauma to the spinal cord results in a primary mechanical insult followed by progressive secondary tissue damage.<sup>1</sup> Whereas secondary injury processes, such as excitotoxicity, ischemia, inflammation, demyelination, and apoptosis, are deleterious, injury to the spinal cord also initiates a number of endogenous restorative responses.<sup>2–4</sup> Among them, 1) angiogenesis, 2) remyelination, 3) transcriptional upregulation of proregenerative genes and 4) neurotrophic factors, 5) axonal regeneration, 6) activation of endogenous antioxidant defenses, and 7) accumulation of prorestorative

fatty acids are well-described spontaneous repair responses post-SCI. Although limited and fragmented, these processes provide a striking example of the spinal cord inherent capacity for tissue repair.

The dietary-essential n-3 polyunsaturated fatty acids (PUFAs) are major components of the neural membrane phospholipids, having important roles in maintaining cell structure, function, and serve as precursors to a myriad of signaling molecules. SCI results in severe perturbations to the metabolism of these fatty acids, particularly docosahexaenoic acid (DHA; C22:6 n-3).<sup>5–8</sup> Our laboratory and others have shown that administration of DHA has polytarget actions and is capable of attenuating secondary damage while promoting functional recovery post-SCI.<sup>9–14</sup> DHA confers

<sup>1</sup>Department of Basic Sciences, Center for Health Disparities and Molecular Medicine, Loma Linda University School of Medicine, Loma Linda, California.

<sup>2</sup>Physiology Department, University of Puerto Rico Medical Sciences Campus, San Juan, Puerto Rico.

strong prophylaxis against functional impairments when supplied before SCI<sup>4,8,13,15,16</sup>; however, the molecular target underlying these repair responses still remains elusive.

Fatty acid binding proteins (FABPs) are abundant cytosolic proteins that function as counterparts to extracellular albumin by binding, transporting, and facilitating the signaling of fatty acids (FAs) and other lipophilic molecules. This family of proteins is currently composed of 10 members and possesses distinctive tissue-specific distribution that may indicate functional differences. The FABP3 (heart type), FABP5 (epidermal type), and FABP7 (brain type) are the main members expressed in the central nervous system (CNS). Emerging evidence demonstrates that CNS FABPs are implicated in neurogenesis,<sup>17</sup> neurotransmission,<sup>18</sup> cognition,<sup>19</sup> and circadian rhythmicity.<sup>20</sup> Interestingly, FABPs exhibit differential binding affinities for PUFAs, resulting in activation of gene transcription and signaling cascades. For instance, the FABP3 binds avidly to the n-6 PUFA arachidonic acid,<sup>21</sup> whereas FABP7 preferentially binds to DHA.<sup>22,23</sup> Notably, the FABP5, which is also referred as keratinocyte- or epidermal-FABP, DA11, and mall, binds both arachidonic acid (AA) and DHA with high affinity.<sup>24,25</sup> This unique binding property suggests that FABP5 may play crucial roles in maintaining adequate n-6 to n-3 PUFA levels and therefore in modulating key restorative and inflammatory signaling pathways.

FABP5 is very abundant in neurons of the retina, hippocampus, cerebellum, and cerebral cortex as well as in motor neurons in the spinal cord during development.<sup>26–28</sup> However, levels of FABP5 decrease during early post-natal periods and remain very low in the adult brain.<sup>29</sup> FABP5 is markedly upregulated in different animal models of neurotrauma, including kainic acid-induced brain injury,<sup>30</sup> peripheral nerve injury,<sup>31</sup> and after cerebral ischemia in primates.<sup>32</sup> We have shown that FABP5 binds to DHA and may be required during neurite outgrowth and cell survival.<sup>25–28,33</sup> Mechanistically, emerging evidence from our lab demonstrates that this protein plays crucial roles in stress responses during lipotoxicity through activation of antioxidant signaling pathways.<sup>34</sup> Here, we investigate the expression and distribution of FABP5 and explore its role in functional recovery after contusive SCI in adult rats.

## Methods

### Animals

Experimental protocols were performed in compliance with Loma Linda University School of Medicine (Loma Linda, CA) and University of Puerto Rico School of Medicine (San Juan, Puerto Rico) regulations and institutional guidelines consistent with the National Institutes of Health (NIH) Guide for the Care and Use of Laboratory Animals. Young-adult female Sprague-Dawley rats were obtained from Hilltop (Scottsdale, PA; used for albumin-DHA experiments) and Charles River Laboratories (Portage, MI; used Western blot, immunohistochemistry, and special diet studies), housed with a light/dark cycle of 12/12 h, and fed *ad libitum*. A cohort of animals was fed custom AIN-93G-based diets that were prepared with alterations to the n-3 FA source as described previously.<sup>4,8</sup> Please refer to Tables 1 and 2 for a detailed description of the composition of the diets. Animals received the diets for 8 weeks before injury and for an additional week post-SCI.

Rats received contusion injuries with the standard New York University/MASCIS impactor weight-drop device.<sup>35</sup> This model simulates most of the biomechanics of human SCI, including changes in gross histological appearance, altered FA metabolism, cell death, and loss of sensorimotor function. Contusion parameters

TABLE 1. DIET COMPOSITION

<i>Ingredient</i>	<i>AIN-93G control diet (%)</i>	<i>AIN-93G fish oil-enriched diet (%)</i>
Casein	20	20
L-cystine	0.3	0.3
Corn starch	39.7	39.7
Maltodextrin	13.2	13.2
Sucrose	10	10
Fiber	5	5
Vitamin mix	1	1
Mineral mix	3.5	3.5
Choline bitartrate	0.25	0.25
tBHQ	0.0014	0.0014
Soybean oil	7	0.77
Fish oil (DHA + EPA + cholesterol)	0	<b>6.23</b>
Cholesterol (added to match fish oil levels)	<b>0.0121</b>	0
% kcal from carbohydrates	64.7	64.7
% kcal from protein	18.8	18.8
% kcal from fat	16.5	16.5
Total kcal	3.77	3.77

tBHQ, tert-butylhydroquinone; DHA, docosahexaenoic acid; EPA, eicosapentaenoic acid.

were not significantly different among the different treatment groups. To perform the surgery, skin and muscles overlying the spinal column were incised and a laminectomy was performed at the thoracic level 10 (T10). Contusions were generated by releasing a weight (10 g, rod diameter of 2 mm) from a height of 12.5 mm on the exposed dura of the spinal cord. Sham animals received only a laminectomy surgery. Post-surgery, muscle layers were sutured and the skin closed with wound clips. Bladders were expressed until voiding reflexes were reestablished. Cefazolin (25 mg/kg, subcutaneously [s.c.]; Bristol-Myers Squibb, New York, NY) and Buprenex<sup>®</sup> (buprenorphine; 0.05 mg/kg, s.c.; Reckitt and Colman Pharmaceuticals, Inc. Richmond, VA) were given to all rats for 5 and 3 consecutive days, respectively. Animals were allowed to survive for 1 week post-surgery.

TABLE 2. DETAILED FA COMPOSITION OF THE DIETS

<i>FA</i>	<i>AIN-93G control diet (g/100-g)</i>	<i>AIN-93G fish oil-enriched diet (g/10-g)</i>
C14:0	0.81	0.50
C16:0	0.32	1.51
C18:0	ND	0.29
Total saturated FA	1.13	2.30
C16:1	0.04	0.68
C18:1	1.57	1.23
Total monosaturated FA	1.61	1.91
C18:2 n-6	3.55	0.55
C18:3 n-3	0.48	0.19
C20:4 n-6	ND	0.08
C20:5 n-3	ND	0.85
C22:5 n-3	ND	0.33
C22:6 n-3	ND	0.56
Total polyunsaturated FA	4.09	2.57

FA, fatty acid; ND, not detected.

### Metabolomics-based lipid analyses

We used standard unbiased metabolic profiling to detect and determine the spinal cord lipid levels, as previously described by our group<sup>4,8,15</sup> and others.<sup>7,36–39</sup> Briefly, animals were deeply anesthetized and transcardially perfused with ice-cold phosphate-buffered saline (PBS). Spinal cord samples (75–100 mg) were dissected and flash frozen in liquid nitrogen. Samples were immediately stored at  $-80^{\circ}\text{C}$  and homogenized in water at the time of analyses. Protein was precipitated with methanol containing four standards to report on the extraction efficiency. The resulting supernatant was split into equal aliquots for analysis on the three platforms. Aliquots were subsequently dried under nitrogen and vacuum desiccated. The metabolomics profiling strategy used for this analysis was based on a combination of three independent platforms: ultra-high-performance liquid chromatography/tandem mass spectrometry (UHPLC/MS/MS<sup>2</sup>) optimized for basic species, UHPLC/MS/MS<sup>2</sup> optimized for acidic species, and gas chromatography/mass spectrometry (GC/MS). Aliquots of a well-characterized human plasma pool served as technical replicates throughout the data set, extracted water samples served as process blanks, and a cocktail of standards added to every analyzed sample allowed for instrument performance monitoring. Experimental

samples and controls were randomized across platform run days. Metabolites were identified by automated comparison of the ion features in the experimental samples and compared to a reference library of chemical standard entries that included retention time, molecular weight ( $m/z$ ), preferred adducts, and fragments as well as associated MS spectra. The detected lipid features were curated by visual inspection for quality control using software developed at Metabolon<sup>® 40</sup>.

### RNA extraction

Intraperitoneal injections of pentobarbital (40–50 mg/kg) were administered to induce euthanasia followed by transcardial perfusion with ice-cold 0.01 M of PBS (pH 7.4; Sigma-Aldrich, St. Louis, MO). Spinal cord segments comprising the lesion epicenter (5 mm) were collected and total RNA was extracted using Trizol reagent (Invitrogen Life Technologies, Carlsbad, CA), according to the manufacturer's instructions. RNA concentration was determined by measuring absorbance at 260 nm on a NanoDrop spectrophotometer (Thermo Scientific, Waltham, MA). We used 800 nanograms of the total RNA for the first-strand complementary DNA (cDNA) synthesis.

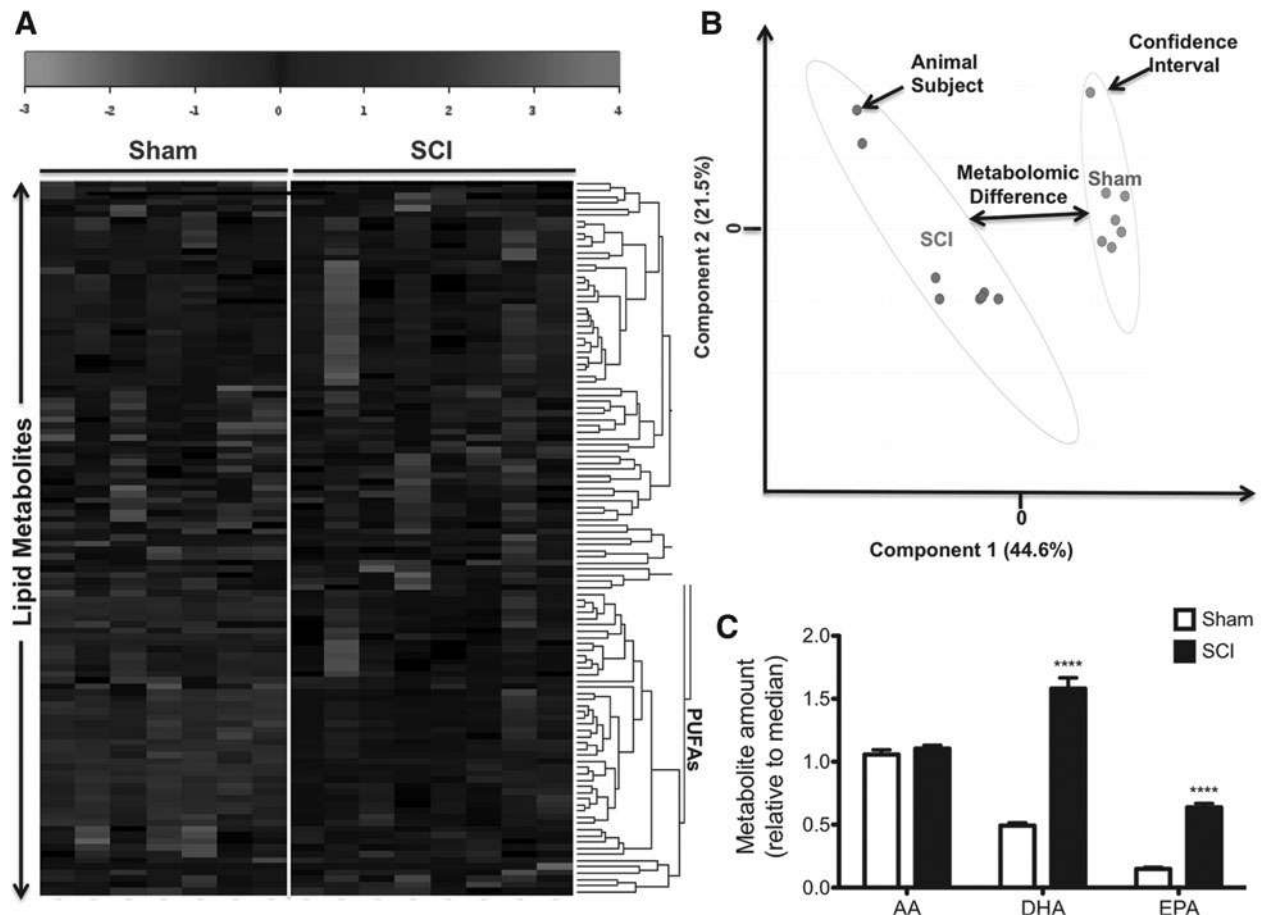


**FIG. 1.** SCI leads to robust alterations to the PUFA neurometabolome during the subacute injury phase. Heatmap representation of unsupervised hierarchical clustering for detected PUFAs (rows) on each sample type (columns) (A). Shades of gray represent metabolite decreases and increases, respectively, relative to the median metabolite levels. See scale. PLS-DA score plot containing two first components (B). Each plot mark corresponds to an observation (individual rat spinal cord sample). The confidence ellipses illustrate the 95% confidence regions. Principal component 1 ( $x$ -axis) shows distinctive spectra between sham and injury groups. SCI led to a significant increase in levels of both DHA and EPA at 7 dpi ( $n$  = at least 7 rats;  $p < 0.05$ ) (C). No changes were observed in levels of AA when comparing sham versus injury groups at 7 dpi ( $p > 0.05$ ). AA, arachidonic acid; DHA, docosahexaenoic acid; dpi, days post-injury; EPA, eicosapentaenoic acid; PLS-DA, partial least squares discriminant analyses; PUFAs, polyunsaturated fatty acids; SCI, spinal cord injury.

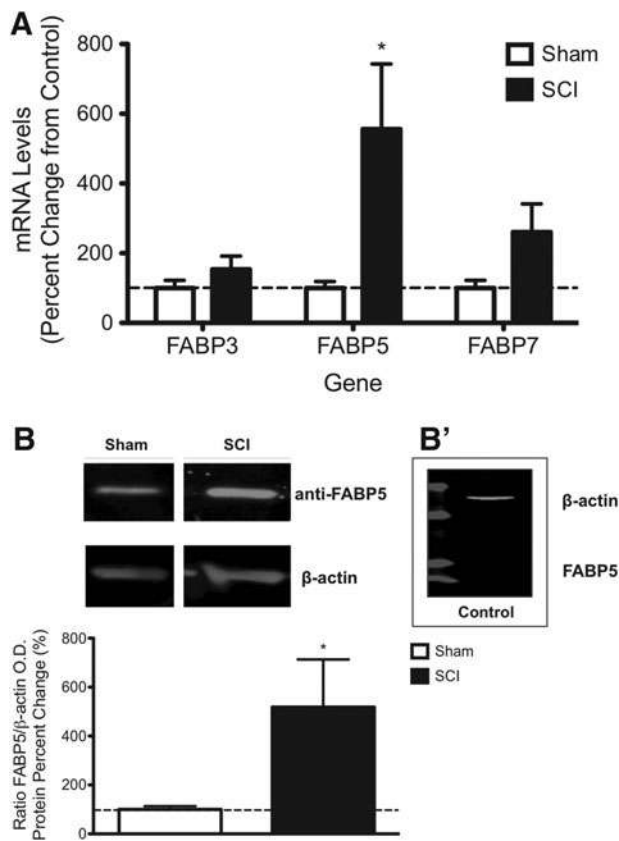


**FIG. 2.** FABP5 expression is induced by contusive SCI. SCI significantly increased levels of FABP5 mRNA levels at 7 dpi ( $p < 0.01$ ) (A). Densitometric analyses of Western blotting showed increased protein levels in SCI rats when compared to sham controls at 7 dpi ( $n =$  at least 6 rats;  $p < 0.05$ ) (B). Pre-bleed serum controls acquired from rabbits used to generate the FABP5 antibody were used to validate the specificity of the immunoreaction (B'). dpi, days post-injury; FABP5, fatty acid binding protein 5; mRNA, messenger RNA; O.D., optical density; SCI, spinal cord injury.

The first-strand cDNA synthesis was primed using oligo (dT) based on the SuperScript II First-Strand synthesis kit (Invitrogen, Carlsbad, CA). The synthesized cDNA was used as a template for estimation of FABP5 transcription in spinal cord tissue by real-time polymerase chain reaction (PCR). cDNA was amplified by PCR using a pair of primers specific for FABP5 (forward [FWD]: 5'-TTA CCC TCG ACG GCA ACA A-3'; reverse [RV]: 5'-CCA TCA GCT GTG GTT TCA TCA-3'); FABP3 (FWD: 5'-AGG TGG CTA GCA TGA CCA AG-3'; RV: 5'-GTC ATC TGC TGT GAC CTC GT-3'); and FABP7 (FWD: 5'-TGT GAC CAA ACC AAC GGT GA-3'; RV: 5'-AGC TTG TCT CCA TCC AAC CG-3'). Glycerol-aldehyde 3-phosphate dehydrogenase (GAPDH; FWD: 5'-TGC CAC TCA GAA GAC TGT GG-3'; RV: 5'-TTC AGC TCT GGG ATG ACC TT-3'), cyclophilin B (FWD: 5'-CTG TCG ATT CCC TCA CAG GT-3'; RV: 5'-AAA ATC AGG CCT GTG GAA TG-

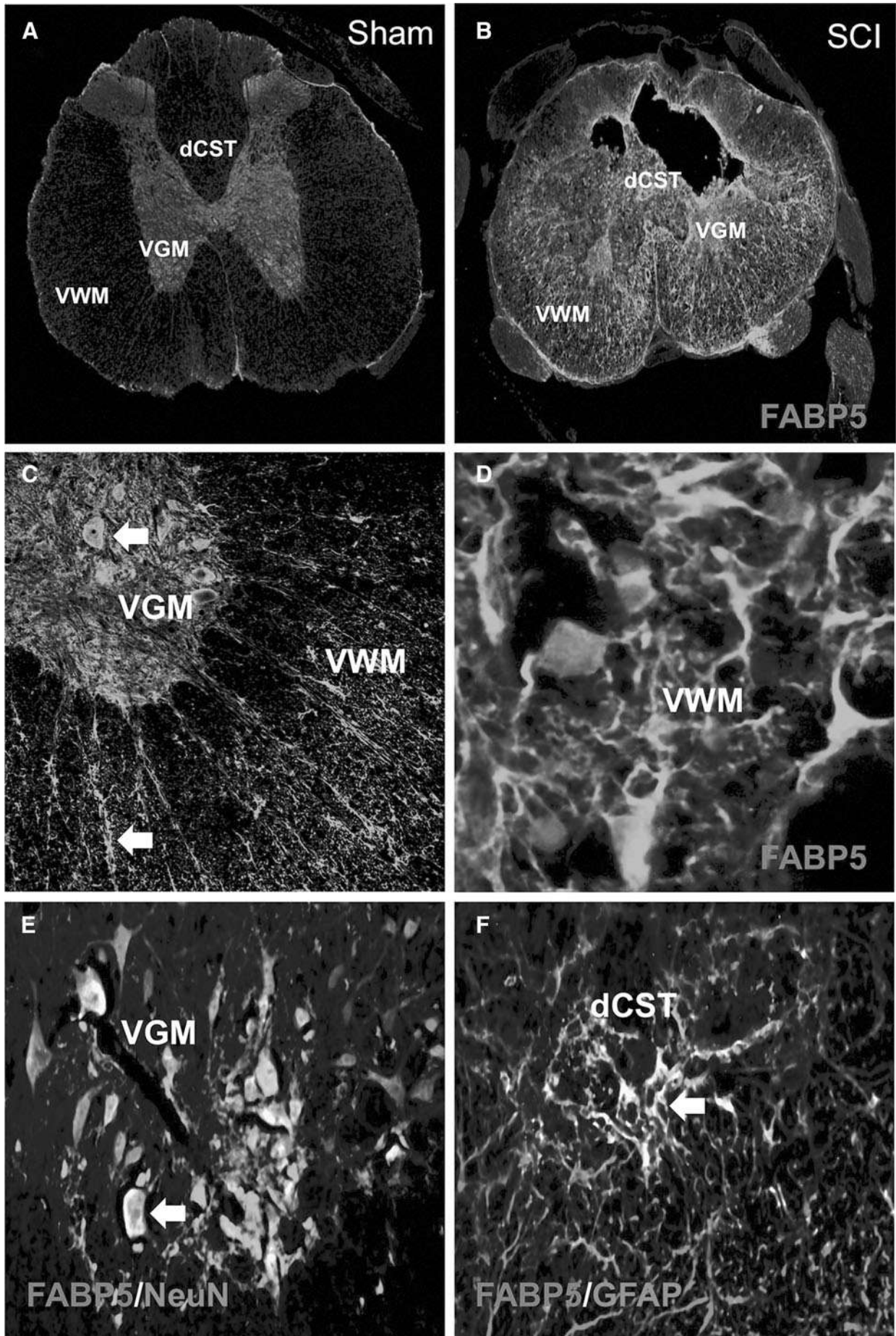
3'), and  $\beta$ -actin (FWD: 5'-GGG AAA TCG TGC GTG ACA TT-3'; RV: 5'-GCG GCA GTG GCC ATC TC-3') served as internal controls for normalization. Real-time PCR amplification and analysis were carried out on a CFX96 Real-Time PCR Detection System (Bio-Rad Laboratories, Hercules, CA). SYBR green I (P/N 4309155; Applied Biosystems, Foster City, CA) was used as a fluorescent reporter dye for the presence of double-stranded DNA. PCR conditions were optimized and 25- $\mu$ L reactions were prepared (SYBR Green PCR Master Mix, 10  $\mu$ M of forward/reverse primer, and 50 ng of cDNA). A negative (mock) control reaction without reverse transcription was included in each experiment, and specificity of the FABP5 PCR product was confirmed by gel electrophoresis and melting curve analysis. A single melting curve peak was used to determine specificity for each additional target gene. Relative levels of FABP3, 5, and 7 messenger RNA (mRNA) were calculated using the comparative Ct (crossing threshold) as previously described.<sup>41</sup> Each sample was normalized to its GAPDH and/or  $\beta$ -actin mRNA content. Relative gene expression levels were normalized to sham animals receiving control diets.

#### Western blot

The spinal cord segment containing the lesion epicenter was dissected and protein extraction performed using adapted protocols from previously published reports.<sup>26,28,42</sup> Briefly, dissected tissue was homogenized in ice-cold lysis buffer (1% Triton X-100, 50 mM of Tris [pH 7.5], 150 mM of NaCl, 5% glycerol, and 1 mM of ethylenediaminetetraacetic acid) with a cocktail of inhibitors contained in complete minitabets (Roche, Indianapolis, IN). After being centrifuged at 20,000g for 10 min, the supernatant (cytosolic) fraction was extracted for analysis. The cytosolic protein concentration was determined using Bio-Rad's DC Protein assay according to the manufacturer's instructions (Bio-Rad Laboratories).

Forty micrograms of protein (40  $\mu$ g) were subjected to a 4–12% gradient sodium dodecyl sulfate polyacrylamide gel electrophoresis (conditions: 45 min, 200 V constant, at room temperature) and electroblotted using nitrocellulose membranes (conditions: 90 min, 35 V constant, at room temperature). All experiments were performed using NuPage Novex<sup>®</sup> pre-cast gels and pre-mixed buffers and the XCell SureLock<sup>™</sup> Mini-Cell System (Invitrogen, Carlsbad, CA). To verify transfer, the nitrocellulose membrane was stained with 0.1% Ponceaus S (in 0.1% glacial acetic acid) for 10 min and then rinsed with 1X Tris-buffered saline (TBS) three times for 10 min each. To reduce background staining, the nitrocellulose membrane was immersed in blocking solution (7.5% nonfat milk, in TBS; pH 7.5) for 2 h at room temperature. The membrane was probed overnight at 4°C with the previously reported rabbit anti-FABP5 serum polyclonal antibody<sup>25</sup> (1:1000) diluted in blocking solution plus 0.1% Tween-20 (1X TBS). Negative control experiments were performed using rabbit pre-bleed serum at the same concentration used to immunodetect FABP5. After, the membrane was washed three times for 10 min each in blocking solution and the secondary antibodies (IRDye 800CW-conjugated donkey anti-rabbit immunoglobulin G [IgG] and IRDye 680-conjugated donkey antimouse IgG; both 1:1,000; LI-COR<sup>®</sup> Biosciences, Lincoln, NE) were applied to the membrane and incubated for 1 h at room temperature. The membrane was washed five times with TBS and Tween 20 and once with TBS for 5 min each. Membrane analysis was performed using the Odyssey<sup>®</sup> Infrared Imaging System (LI-

**FIG. 3.** FABP5 is mostly expressed by neurons in sham animals and in glia in the injured spinal cord. Basal levels of FABP5 expression were detected in the spinal cord gray matter (A). Increased FABP5 immunoreactivity was observed in spinal cord ventral white (VWM) and gray matter (VGM) at 7 dpi (B). Interestingly, this expression was more prominent in neuron- and glial-like cells (C and D). Confocal imaging definitively colocalizes FABP5 to neurons (NeuN<sup>+</sup>) (E) and activated astrocytes (GFAP<sup>+</sup>) (F); see arrows. Scale bars: 20  $\mu$ m. dCST, dorsal corticospinal tract; dpi, days post-injury; FABP5, fatty acid binding protein 5; GFAP, glial fibrillary acidic protein; NeuN, neuronal nuclei.



COR® Biosciences). Relative levels of FABP5 protein were normalized to the amount of  $\beta$ -actin in each sample.

### Histology and neuroimaging

To prepare tissue for confocal immunofluorescence analyses, we followed previously published procedures.<sup>13</sup> Briefly, animals were submitted to fast and humane euthanasia with Fatal-Plus™ (Vortech, Dearborn, MI) and perfused transcardially with PBS, followed by 4% paraformaldehyde (PFA) in 0.1 M of phosphate buffer.

Spinal cord segments containing the lesion epicenter were removed and post-fixed for 3–5 h in 4% PFA, cryoprotected in 30% sucrose for 12–16 h at 4°C, embedded in Tissue-Tek® O.C.T.™ compound (Sakura, Torrance, CA), and immediately frozen on dry ice. A series of transverse 20- $\mu$ m cryodissections were cut on a Richart-Jung Cryocut 1800 cryostat (Leica, Deerfield, IL) and placed on consecutive microscope slides (Superfrost Plus; Fisher Scientific, Pittsburgh, PA) so that each slide contained representative sections from rostral, epicenter, and caudal regions. Spinal cord sections were dried at room temperature for 10–15 min, washed with PBS, and post-fixed with 4% PFA for 10 min. Immunofluorescence double labeling has been described in previous work.<sup>15</sup> In brief, a mixture of our custom rabbit polyclonal anti-rFABP5<sup>28</sup> (1:500) and mouse anti-NeuN (neuronal nuclei; 1:500; Millipore, Temecula, CA), anti-NFH (neurofilament heavy polypeptide; 1:500; Millipore, Temecula, CA), anti-GFAP (glial fibrillary acidic protein; 1:500; Millipore, Temecula, CA), anti-CC1 (allophycocyanin [APC]-7; 1:350; Calbiochem, San Diego, CA), or anti-CD68 (1:400; AbD Serotec, Raleigh, NC) antibodies were used to examine colocalization of FABP5 in neurons, axons, astrocytes, oligodendrocytes, or macrophages, respectively. Paired antibody solutions were applied to sections overnight at 4°C. On the following day, sections were incubated with Alexa Flour® 488-conjugated donkey antirabbit (1:250; Invitrogen) and Alexa Flour 594-conjugated donkey antimouse (1:250; Invitrogen) antibodies. Primary antibody omission controls and pre-bleed serum controls were used to further confirm the specificity of the immunofluorescence double labeling. At least five sections per spinal cord were examined under confocal laser scanning microscope (FV1000, Olympus or LSM710; Carl Zeiss GmbH, Jena, Germany) or fluorescence microscope (BZ9000; Keyence Corporation, Osaka, Japan). Images were analyzed using ImageJ software (NIH, Bethesda, MD) or BZ-II Analyzer and prepared for publication with Photoshop CS4 software (Adobe Systems, San Jose, CA).

### Behavioral evaluation of spontaneous locomotion

Spontaneous open-field locomotion was evaluated using the 22-point Basso-Beattie-Bresnahan (BBB) locomotor scale.<sup>45</sup> Animals were acclimatized to the open-field environment during several sessions before testing. Testing sessions were videotaped and evaluated as previously reported.<sup>8,13</sup> Two blinded observers assessed the footage and scored the locomotive function (i.e., joint movement, paw placement and rotation, coordination, and tail and trunk position and stability). Briefly, scores range from 0 (flaccid paralysis) to 21 (normal gait). The rating scale involves hindlimb movement (scores range, 0–7) and weight support with/without coordination (scores range, 8–13), which is a major improvement in

recovery. BBB scores higher than 13 are extremely rare at 1 week post-contusion. These scores represent constant forelimb-hindlimb coordination and the appearance of fine motor skills.

### Docosahexaenoic acid/albumin complex

DHA was complexed to human serum albumin (BUMINATE 25%; Baxter, Deerfield, IL). Buminate is manufactured from human plasma by the modified Cohn-Oncley cold ethanol fractionation process, which includes a series of cold-ethanol precipitation, centrifugation, and/or filtration steps followed by pasteurization of the final product at 60±0.5°C for 10–11 h. This process accomplishes both purification of albumin and reduction of viruses. DHA was complexed to human albumin by incubating 20 mL of human serum albumin (25%; Baxter) with 4.0 mg of DHA/g of albumin (molar ratio, 0.2) in a shaking incubator at 37°C for 30 min with vortex mixing every 5 min. A previous report showed that this formulation leads to 2.1±0.1  $\mu$ mol DHA/mL of albumin.<sup>44</sup>

### Small interfering RNA preparation and dosing

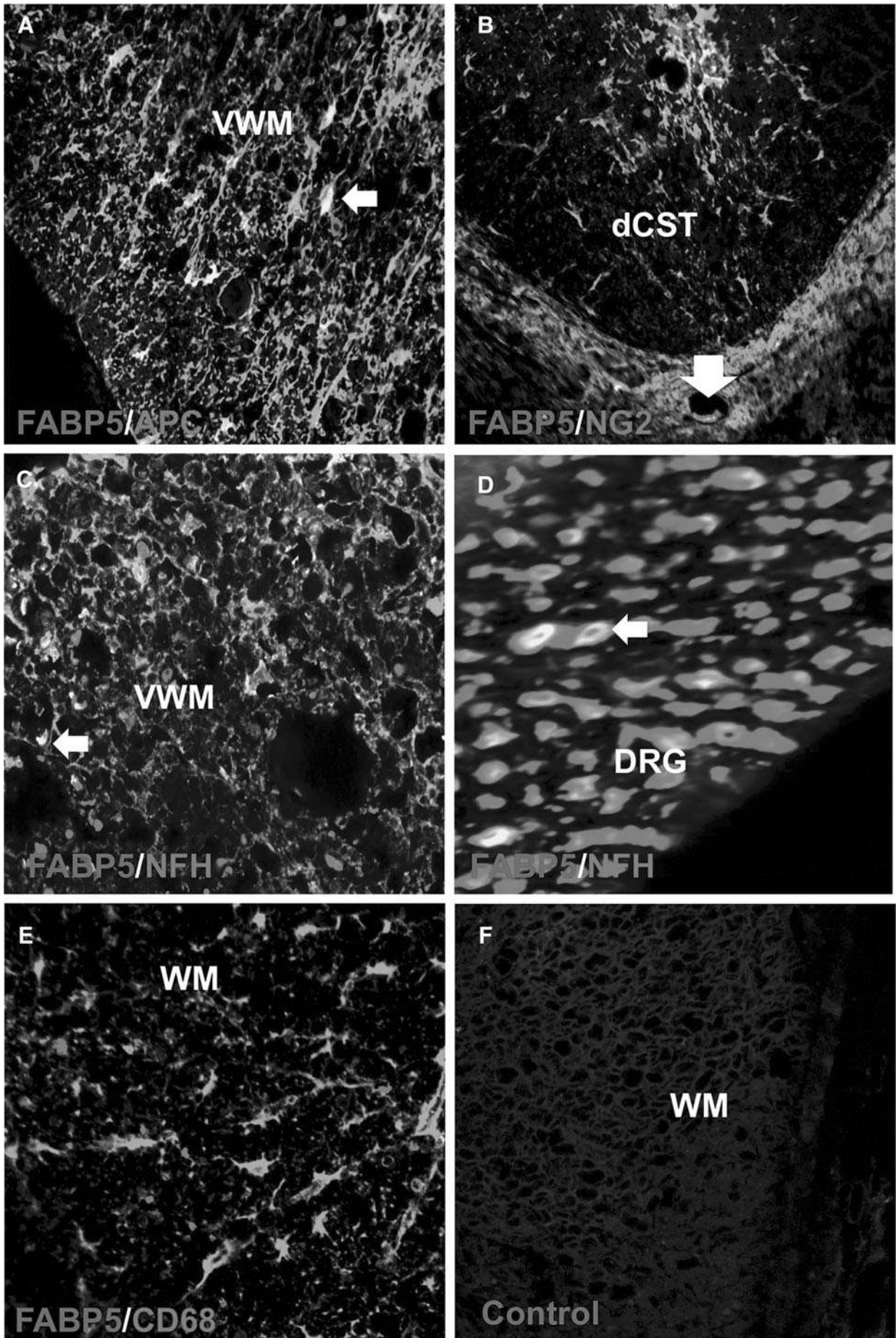
FABP5 siRNA stock solutions (100  $\mu$ M) were prepared in RNase-free reconstitution buffer and stored in aliquots at –80°C. In these experiments, we used a siRNA pool mixture (Smart pool siRNA; pool no.: M-120235-00; Dharmacon Inc.; Chicago, IL). The siSTABLE-modified nontargeting double-stranded RNA was used as controls (no. D-001700-01-20; Dharmacon, Lafayette, CO). The siGLO® green fluorescent oligonucleotides were used as transfection indicators, thus permitting unambiguous visual assessment of uptake into cells. Positive control experiments were performed codelivering siGLO and/or functional cyclophilin B siRNA (ON-TARGETplus™ control siRNA, 1:1 ratio; 50 nM each; Dharmacon). FABP5 siRNA dose-response titration was accomplished using varying doses of oligonucleotides (ranging from 0.5 to 2  $\mu$ g). These were delivered locally into the spinal cord of naïve and injured rats by intraspinal injections or intrathecal catheters attached to an osmotic minipump. To facilitate delivery and uptake, siRNA aliquots were mixed (1:5, v/v) with the cationic lipid based transfection reagent i-Fect™ (Neuromics, Edina, MN).

### Injections

A group of animals were placed in a Digital Lab Standard™ stereotaxic frame (Stoelting, Wood Dale, IL) and received intraspinal injections containing the FABP5 siRNA. Injections were performed in anesthetized rats using the stereotaxic spinal adapter and clamping system. The custom-made glass micropipette (external diameter = 25–35  $\mu$ m; Clunbury Scientific, LLC; Bloomfield Hills, MI) was filled with the oligos and iFect (Neuromics) transfection reagent and attached to a Hamilton® syringe connected to a micromanipulator. The tip of the micropipette was lowered into the spinal cord and intraspinal injections were made bilaterally according to the following stereotaxic coordinates (from midline medial-lateral [ML] to dorsal-ventral [DV]; 0.25  $\mu$ L per injection): 1) 0.7 mm ML, –1.5 mm DV; 2) 0.7 mm ML, –1.3 mm DV; 3) 0.7 mm ML, –0.9 mm DV; and 4) 0.7 mm ML, –0.6 mm DV. siRNA dose and volume selected was based on previous works.<sup>41,45,46</sup> After each injection, siRNA was allowed to disperse over a 2-min period and the micropipette slowly withdrawn. After

**FIG. 4.** FABP5 immunoreactivity is mostly observed in glial cells post-SCI. FABP5 immunoreactivity was detected in oligodendrocytes (A) and precursor cells expressing the NG2 proteoglycan (B). Immunofluorescence photomicrographs revealed FABP5 protein expression in axons and cytoskeletal structures of the VWM (C) and DRG (D). FABP5 was not expressed in macrophages/monocytes (CD68) (F). Pre-immunization serum confirmed the specificity of the immunoreaction (G). Scale bars: 20  $\mu$ m. APC, allophycocyanin; dCST, dorsal corticospinal tract; DRG, dorsal root ganglion; FABP5, fatty acid binding protein 5; NFH, neurofilament heavy polypeptide; NG2, neuron-glia antigen 2; SCI, spinal cord injury; VWM, ventral white matter; WM, white matter.





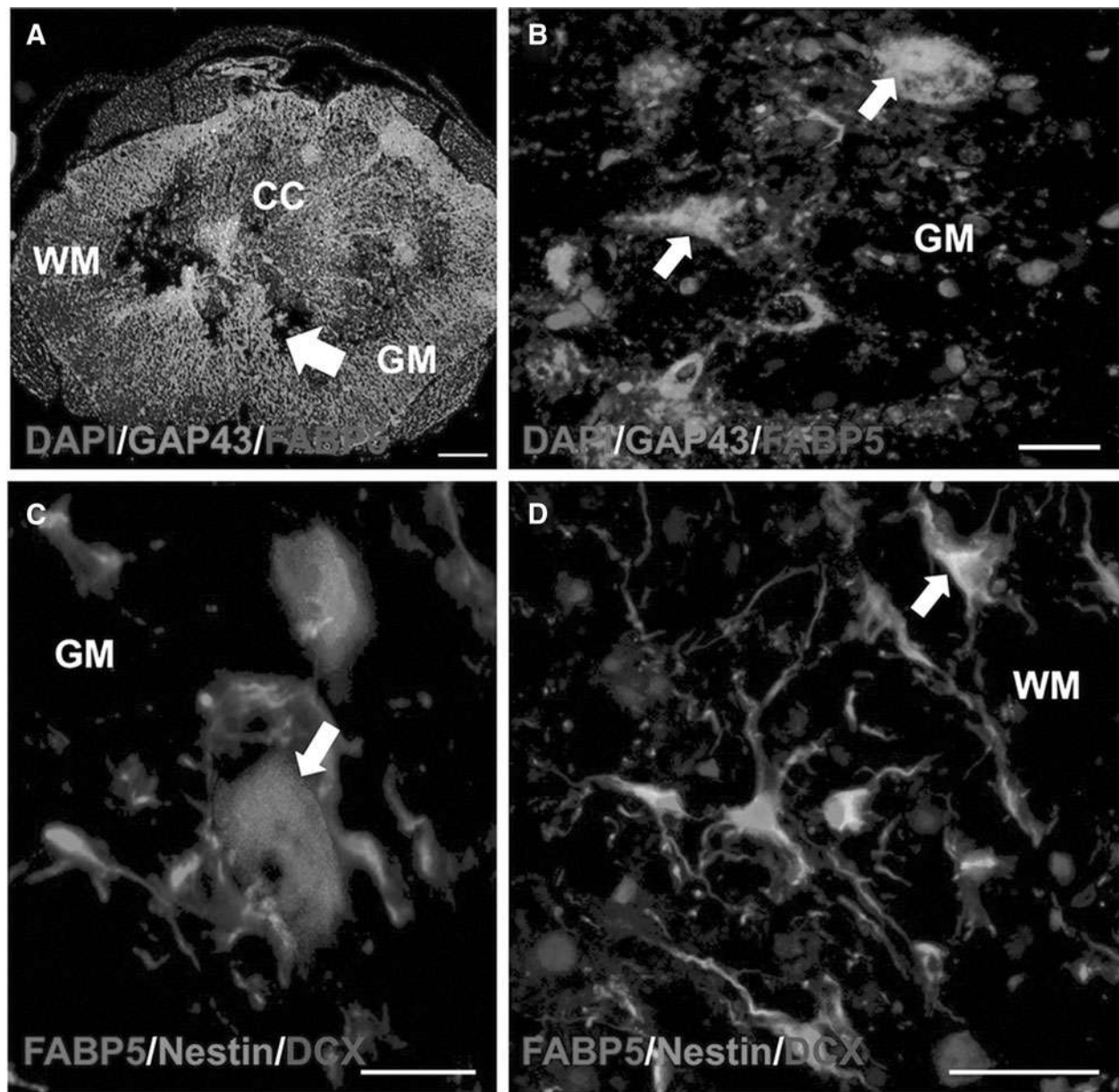


**FIG. 5.** FABP5 expression is prominent in sprouting fibers and neural stem cells post-SCI. Confocal microphotographs show that FABP5 protein colocalized with cells and structures that were positive to the growth-associated protein 43 (GAP43<sup>+</sup>) (A and B). Notably, we observed FABP5 expression in neurogenic niches post-SCI, as evidenced by colocalization of FABP5 to GM cells positive to doublecortin (DCX) (C) and WM cells immunoreactive to nestin (D). Scale bars: 20  $\mu$ m. DAPI, 4',6-diamidino-2-phenylindole; FABP5, fatty acid binding protein 5; GM, gray matter; SCI, spinal cord injury; WM, white matter.

suturing muscle and skin layers, animals were allowed to recover in heating pads and then returned to the animal care facility. Rats were sacrificed 72 h after the injections and the total RNA was collected from spinal cords.

#### Minipumps

In another set of experiments, animals received a second narrow laminectomy between the T11 and T12 level to expose the spinal cord, as previously reported.<sup>41</sup> The dura was carefully punctured with a 27- to 32-gauge needle, raised with fine forceps, and cut with scissors avoiding damage to the spinal cord. A small s.c. pocket was made over the sacral vertebrae caudal to the incision, and a primed Alzet<sup>®</sup> osmotic minipump (model 2001D; 1- $\mu$ L infusion per hour

over 7 days; DURECT Corp., Cupertino, CA) was placed in the pocket with the pump flow moderator facing the incision. Pumps were primed with DHA-albumin complex (DHA), FABP5 siRNA, and vehicle controls. Control pumps were filled with the scramble nontargeting oligos or ethanol vehicle. Animals did not show any noticeable signs of hypersensitivity or distress during the infusion period. The intrathecal catheter, consisting of sterile 28-G polyurethane tubing (Alzet<sup>®</sup>; P/N 000740-1), was inserted through the punctured dura and placed in the lesion epicenter. Tubing was attached to the fascia over the paravertebral muscles at the incision margin, secured with Krazy Glue (Elmer's Products Inc., Columbus, OH) onto the proximal portion of the T13–T14, and reinforced with sutures. Muscle and skin layers were closed after the surgery. The surgeon lacked knowledge of the experimental groups.



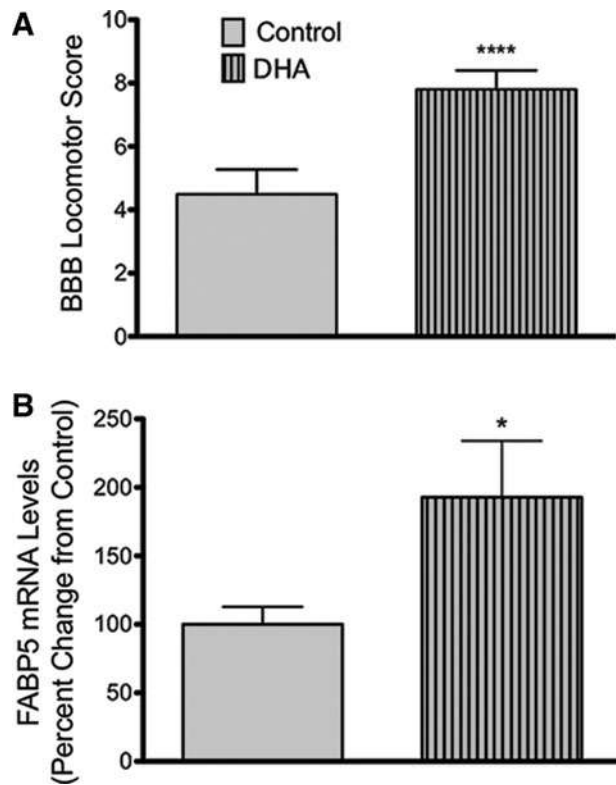


**FIG. 6.** FABP5 is markedly upregulated at 7dpi in animals fed DHA-rich diets. Injured rats consuming diets rich in DHA for 8 weeks pre-injury and 7 days post-injury showed improved locomotor recovery when compared to animals receiving control diets at 7 dpi ( $n =$  at least 24 animals;  $p < 0.0001$ ) (A). Animals with a DHA-enriched diet presented an increased in levels of FABP5 mRNA expression when compared to injured animals receiving control diets ( $n =$  at least 7 rats;  $p < 0.05$ ) (B). BBB, Basso-Beattie-Bresnahan locomotor scale; DHA, docosahexaenoic acid; dpi, days post-injury; FABP5, fatty acid binding protein 5; mRNA, messenger RNA.

#### Statistical analysis

Data are expressed as the mean  $\pm$  standard error of the mean (SEM), and statistical analysis was performed by repeated measures and two-way analysis of variance (ANOVA). Bonferroni's multiple comparison post-hoc test was used to compare differences among samples. All other data were assessed by Mann-Whitney's *U* test, unless stated otherwise. MetaboAnalyst ([www.metaboanalyst.ca](http://www.metaboanalyst.ca))<sup>47</sup>, and the 'R' program (<http://cran.r-project.org/>) were used to analyze the metabolomics data sets. Unsupervised hierarchical clustering was used to generate heat maps. Partial least squares discriminant analyses (PLS-DA) were obtained using the variation scores of the first two principal components. The point marks in the plot represent the variability in relative lipid metabolite levels detected for each animal. Hotelling's  $T^2$  confidence ellipse, at a significance level of 0.05, revealed no outliers following autoscaling. Differences were considered to be significant when  $p < 0.05$ .

## Results

### *Injury to the spinal cord results in a marked perturbation to the metabolism of polyunsaturated fatty acids*

To test the hypothesis that contusive SCI results in lipid deregulation during the subacute phase at 1 week post-injury, we analyzed the spinal cord lipid profile using both LC/MS and GC/MS. Heatmaps

revealed marked differences in lipid profiles between groups (Fig. 1A). We found increased levels of PUFAs in spinal cord tissue of injured animals at 7 days post-injury (dpi). PLS-DA revealed significant metabolomic separations between sham and injured groups at 7 dpi ( $p < 0.05$  by permutation test; data not shown; Fig. 1B).

We found that levels of n-3 PUFAs in the spinal cord had a robust contribution to the metabolomic differences observed. In particular, levels of DHA and EPA were significantly increased at 7 dpi ( $n = 7-8$  rats per group;  $p < 0.05$ ). Unexpectedly, no significant changes were observed in spinal cord levels of the n-6 PUFA, AA, when compared to sham rats at 7 dpi ( $p > 0.05$ ).

### *Spinal cord injury increases the messenger RNA and protein levels of fatty acid binding protein 5*

Because of the hydrophobicity of n-3 PUFAs, their intracellular transport and signaling may be facilitated by FA binding proteins in the cytoplasm. To determine expression levels of FABPs, we measured mRNA levels of the main FABPs using quantitative real-time PCR (qRT-PCR). Although there was a slight tendency for increased expression, we found no significant changes in mRNA levels of FABP3 and FABP7 post-SCI when compared to sham controls at 7 dpi ( $p > 0.05$ ). Notably, FABP5 mRNA levels were significantly upregulated at 7 dpi (556  $\pm$  187% increase; mean  $\pm$  SEM;  $n = 7-8$  rats;  $p < 0.01$ ; Fig. 2A), suggesting a potential role for this protein gene in lipid metabolism and signaling after PUFA accumulation in SCI rats.

We used Western blotting to confirm that FABP5 mRNA is translated into protein post-SCI. Whereas immunoblotting with the anti-FABP5 antibody detected a single 15-kDa peptide in rat spinal cords extracts (Fig. 2B), no immunoreactivity was observed when we replaced the primary antibody with the pre-bleed serum controls acquired from the rabbits used to generate the FABP5 antibody (Fig. 2B'). This finding validated the specificity of the immunoreaction. Our densitometric analyses revealed a 518  $\pm$  195% increase in FABP5 protein levels when compared to sham controls at 7 dpi ( $n = 6-7$  rats;  $p < 0.05$ ; Fig. 2B). No significant FABP5 protein changes were observed between SCI and sham rats at 1 and 3 dpi (data not shown). No significant changes were observed in  $\beta$ -actin levels between groups ( $p > 0.05$ ).

### *Fatty acid binding protein 5 immunoreactivity is observed in spinal cord neurons and glia*

We found very low basal expression of FABP5 in spinal cord of sham animals, which was mostly localized in the gray matter (GM; Fig. 3A). In contrast, SCI rats showed a robust increase in immunoreactivity to FABP5 after injury (Fig. 3B). Higher magnification photomicrographs revealed expression of FABP5 in neuron- and glial-like cells (Fig. 3C,D).

Double-labeling immunostaining for FABP5 and NeuN showed selective expression of FABP5 in distinct ventral motor neuron populations in regions distal (>2.5 mm) from the lesion epicenter (Fig. 3E). FABP5 immunoreactivity was observed in reactive astrocytes in the dorsal corticospinal tract (dCST) and ventral white matter (VWM) of contused spinal cord (Fig. 3F). We found FABP5 expression in oligodendrocytes and putative oligodendrocyte precursor cells, as evidenced by FABP5<sup>ir</sup> in APC<sup>+</sup> (Fig. 4A) and neuron-glial antigen 2 (NG2)<sup>+</sup> (Fig. 4B) cells, respectively. Double immunofluorescence revealed FABP5 expression in axons and cytoskeletal structures of the VWM (Fig. 4C) and dorsal root ganglion (Fig. 4D) at 7 days post-SCI. Colocalization of FABP5 with the macrophage marker, CD68<sup>+</sup>, was not observed (Fig. 4F).

Incubations replacing the primary antibody with pre-immunization serum confirmed the specificity of the immunoreaction (Fig. 4G).

*Fatty acid binding protein 5 is highly expressed in neural precursor cells after spinal cord injury*

We investigated expression of FABP5 in neural precursor cells and structures associated with regeneration and repair using triple-labeling immunohistochemistry. Interestingly, we found that FABP5 expression colocalized with cells and structures that are positive to the growth-associated protein 43 (GAP43; Fig. 5A,B). We also observed a large subpopulation of doublecortin<sup>+</sup> and nestin<sup>+</sup> cells expressing FABP5, suggesting its potential as a biomarker for neurogenesis. This validates our previous observations, which demonstrated that FABP5 expression is important for neurite outgrowth.<sup>25</sup>

*A prorestorative diet rich in docosahexaenoic acid increases the messenger RNA levels of fatty acid binding protein 5 after spinal cord injury*

In agreement with our previous published observations, we found that a diet rich in DHA significantly improved functional recovery at 7 dpi (Fig. 6A;  $n$ =at least 24 animals;  $p<0.0001$ ). Interestingly, animals fed the DHA-enriched diets for 8 weeks before SCI showed higher levels of FABP5 mRNA expression at 7 dpi when compared to injured animals receiving control diets ( $p<0.05$ ; Fig. 6B). Although the diet rich in DHA did not affect mRNA levels of FABP3, we found a slight, yet significant, decrease in the levels of FABP7 in animals fed DHA-enriched diets when compared to animals fed control diets at 7 dpi (data not shown).

*Fatty acid binding protein 5 small interfering RNA penetrates spinal cord cells and blocks fatty acid binding protein 5 expression levels*

To assess the functional significance of FABP5 in SCI, we administered a rat sequence-specific siRNA to attenuate FABP5 mRNA levels. To demonstrate diffusion of the intrathecally infused oligodeoxynucleotides (ODNs), a group of injured animals were treated with ODNs conjugated with fluorescein isothiocyanate (FITC). Spinal cords were dissected out and sectioned to visualize ODN diffusion 1 week post-implantation. We found that fluorescence of the tagged ODNs was noticeable near caudal regions from the infusion site (Fig. 7A). We observed that labeled ODNs were incorporated in spinal cord cells, as evidenced by FITC colocalization with 4',6-diamidino-2-phenylindole (DAPI) staining (Fig. 7B). Spinal cord sections from animals receiving nontagged ODNs showed no fluorescence (Fig. 7C). We have extensively validated the efficacy of this siRNA sequence to block FABP5 protein expression.<sup>25</sup> Here, we found that intrathecal FABP5 siRNA administration resulted in a 60% reduction in mRNA levels of FABP5 ( $p<0.05$ ; Fig. 7D). In contrast, the nontargeting scramble sequence did not perturb FABP5 mRNA levels, demonstrating that FABP5 siRNA was both sequence and target specific. Representative Western blot shows the efficacy of this sequence to block FABP5 protein expression (Fig. 7E)

*Fatty acid binding protein 5 small interfering RNA administration hinders locomotor recovery after spinal cord injury*

A key finding of this study is that animals receiving FABP5 siRNA showed a transient impairment in locomotor recovery at

5 dpi when compared to animals receiving the scrambled control ODNs sequence ( $p<0.05$ ; Fig. 8). Similarly, concomitant intrathecal administration of DHA and FABP5 siRNA hindered the beneficial effects of this FA to promote locomotor recovery at 7 dpi ( $p<0.05$ ).

## Discussion

This study demonstrates that acute SCI leads to perturbations to the metabolism of n-3 PUFAs. We show that SCI also induces a robust upregulation in mRNA levels and protein expression of FABP5. This study reveals that FABP5 levels are sensitive to dietary n-3 PUFAs found in fish oils. Post-SCI, we found high levels of FABP5 in glial and neural precursor cells associated with repair processes. We show that FABP5 blockade impairs spontaneous locomotor recovery post-SCI. Notably, administration of FABP5 siRNA interfered with the ability of DHA to restore extensive hindlimb movements and weight support stepping at 1 week post-injury. Altogether, the findings presented herein suggest that FABP5 plays a role in the pathophysiology of SCI and may be implicated in functional recovery through the cellular uptake and mobilization of n-3 PUFAs, particularly DHA.

*Spinal cord injury leads to marked derangements in n-3 polyunsaturated fatty acid metabolism*

In agreement with a growing body of studies, this study demonstrates that metabolism of n-3 PUFAs may play important roles in the endogenous protective responses activated after traumatic brain injury and SCI.<sup>4,16,48,49</sup> Although the available evidence supports an important role for n-3 PUFAs in inflammation, neuroprotection, neurogenesis, and plasticity, the mechanisms involved in their incorporation and metabolism are largely unknown and warrants further examination for successful clinical translation.<sup>50</sup>

*Fatty acid binding proteins regulate n-3 polyunsaturated fatty acid trafficking and metabolism*

Intracellular PUFAs bind to cytoplasmic FABPs. These small proteins are believed to promote cellular uptake and transport of PUFAs, targeting of FAs to specific metabolic pathways, and actively participate in regulation of gene expression as well as cell proliferation and growth.<sup>51</sup> Among the FABP family, only three subtypes are expressed in the CNS: the FABP3 (heart type); FABP5 (epidermal type); and FABP7 (brain type). These FABPs are believed to be important in neurogenesis and have been recently implicated in the pathophysiology of several neural and psychiatric disorders.<sup>52–55</sup> Interestingly, each FABP possesses a distinctive cell expression profile and binding affinity for different PUFAs.<sup>21–24</sup> Long-standing evidence supports the idea that FABPs, particularly FABP3, may maintain phospholipid pool mass and acyl chain composition.<sup>56,57</sup> A previous report from our group has shown that FABP5 can bind the n-6 PUFA, AA, and the n-3 PUFAs, DHA, and EPA with very high affinity.<sup>25</sup> This unique binding property suggests that FABP5 may have an essential role in maintaining the cellular n-6/n-3 PUFA ratio, an important biomarker of functional recovery in brain- and spinal cord-injured rats.<sup>8,58</sup> Further, structural analysis of rat FABP5 reveals five cysteine residues and one major disulfide bond with high binding affinity for 4-hydroxynonenal and reactive oxygen species, and emerging findings from our laboratory propose a role for this protein in promoting antioxidant mechanisms.<sup>34,59,60</sup>

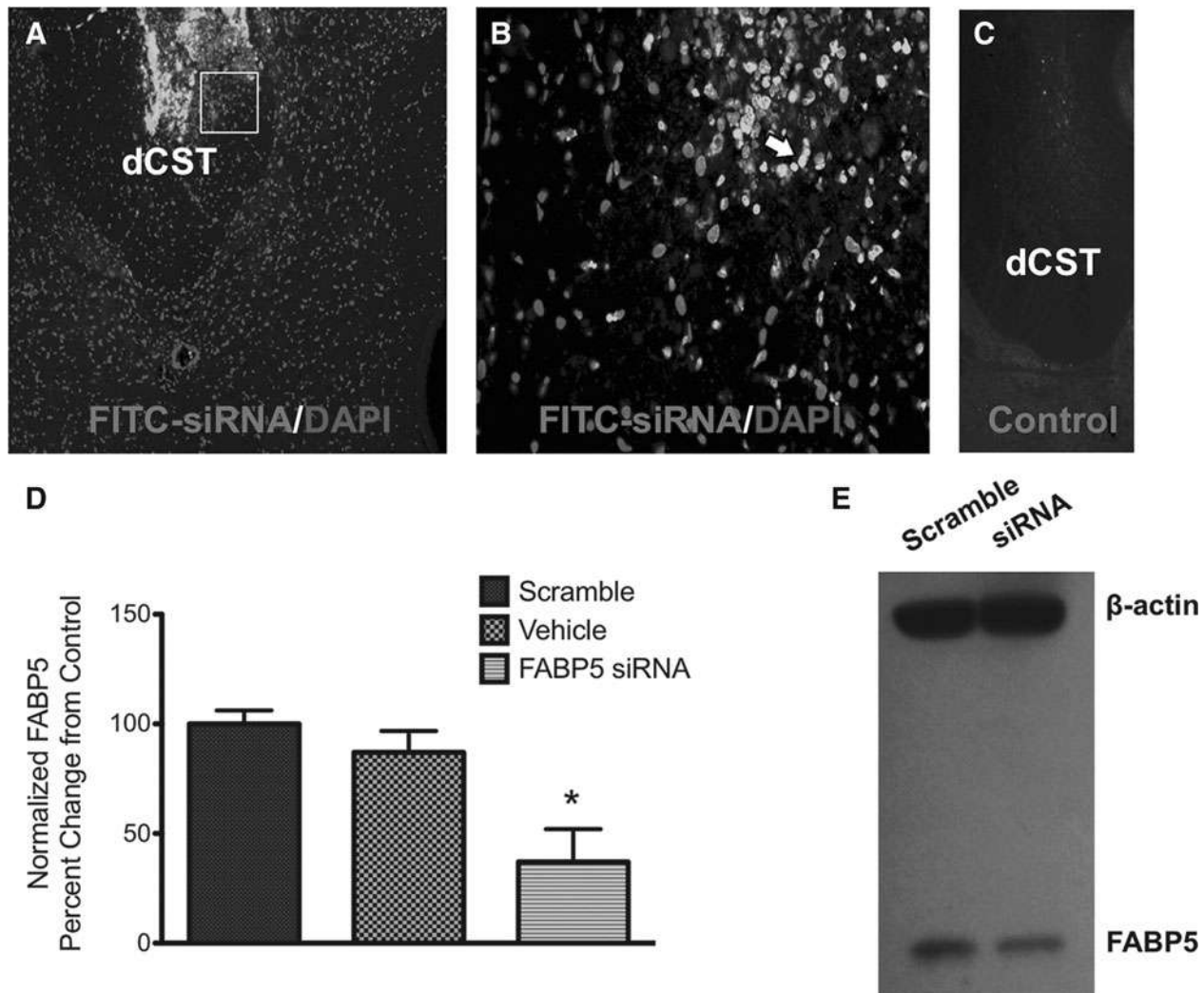


**FIG. 7.** FABP5 siRNA penetrates injured spinal cord and blocks FABP5 mRNA and protein expression. Photomicrograph of spinal cord section from an animal receiving intrathecal FITC-tagged siRNA demonstrates penetration of oligonucleotides (A). Confocal microscopy revealed that most staining was localized in cells of the dorsal white matter in the CST area (B). Fluorescence was absent in the spinal cord sections from animals receiving non-FITC-tagged ODNs (C). qRT-PCR analysis of FABP5 siRNA-treated spinal cords showed a 60% reduction in FABP5 mRNA levels relative to animals treated with control scrambled sequence oligonucleotides ( $n =$  at least 3 animals per group;  $p < 0.05$ ) (D). As recently reported,<sup>33</sup> immunoblotting of cells treated with FABP5 siRNA showed reduced protein levels (E). CST, corticospinal tract; DAPI, 4',6-diamidino-2-phenylindole; dCST, dorsal corticospinal tract; FABP5, fatty acid binding protein 5; FITC, fluorescein isothiocyanate; mRNA, messenger RNA; ODNs, oligodeoxynucleotides; qRT-PCR, quantitative real-time polymerase chain reaction; siRNA, small interfering RNA.

Previous studies demonstrate the upregulation of FABP5 in different models of neural injury.<sup>30–32,61–63</sup> In agreement with these findings, we demonstrate that FABP5 expression increases in SCI rats. Interestingly, we found that this response was selective to FABP5 given that SCI did not induce significant changes in mRNA levels of FABP3 and FABP7 at 7 dpi. Although our study did not rule out that other FABPs play a role in the pathophysiology of SCI, the robust induction of FABP5 expression post-injury suggests that this protein may be a mediator of lipid transport and metabolism during injury periods, characterized by active cell membrane turnover and proliferation.

During development, FABP5 is very abundant in cells with high metabolic activity, including neurons in the retina, hippocampus, cerebellum, and cerebral cortex as well as motor neurons in the spinal cord.<sup>26–28</sup> Expression of FABP5 is also evident in astrocytes and radial glia of the rodent brain, but decreases after birth.<sup>29,64</sup>

Here, we found a subpopulation of motor neurons that were positive to FABP5, mostly in regions proximal to the injury site post-SCI. We observed very low FABP5 levels in neurons of the lesion epicenter, possibly reflecting an altered metabolic state of the GM that results in cell loss post-injury. The marked colocalized expression pattern of FABP5 with glial cells during the subacute phase of injury supports their role as reservoirs and facilitators of FA transport and metabolism. Our data are in agreement with studies in mice showing increased levels of FABP7 in GFAP<sup>+</sup> astrocytes at 7 days post-injury to the spinal cord<sup>65</sup> or brain.<sup>66</sup> Evidence demonstrates that astrocytes have the ability to synthesize n-6 and n-3 elongation products.<sup>67,68</sup> Together, it is thus plausible that FABPs may facilitate DHA supply to neurons and influence neural metabolism and synaptic activity after neurotrauma.

FABP5 is expressed at high levels during neurogenesis, neuronal migration, and differentiation.<sup>26,27,29</sup> Further, FABP5 is highly

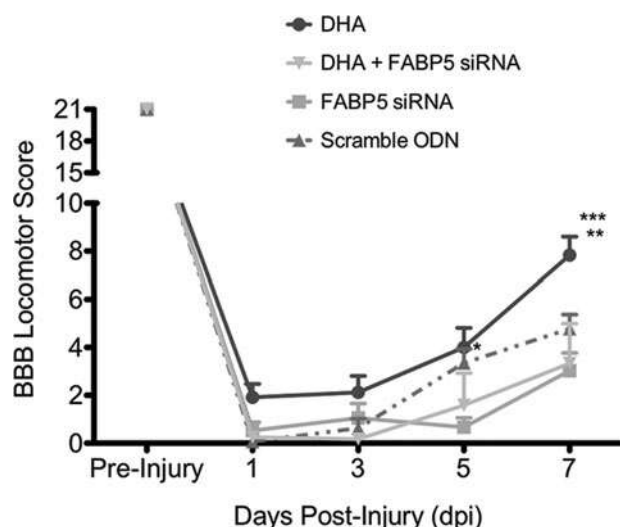


**FIG. 8.** FABP5 siRNA administration hinders locomotor recovery post-SCI. BBB locomotor scores were obtained every other day for 1 week post-SCI. Administration of  $2\ \mu\text{g}$  of FABP5 siRNA showed a transient impairment in locomotor recovery at 5 dpi when compared to animals receiving scrambled sequence oligos ( $n=8-9$  animals per group; two-way ANOVA;  $p<0.01$ ). Notably, concomitant administration of DHA and FABP5 siRNA abolished the beneficial effects of DHA to accelerate locomotor recovery at 7 dpi ( $n=3-6$  animals per group; two-way ANOVA;  $p<0.001$ ). \* $p<0.05$  when comparing FABP5 siRNA versus control at 5 dpi; \*\* $p<0.001$  when comparing DHA versus control at 7 dpi; \*\*\* $p<0.0001$  when comparing DHA versus DHA + FABP5 siRNA at 7 dpi. ANOVA, analysis of variance; BBB, Basso-Beattie-Bresnahan locomotor scale; DHA, docosahexaenoic acid; dpi, days post-injury; FABP5, fatty acid binding protein 5; FITC, fluorescein isothiocyanate; ODN, oligodeoxynucleotide; SCI, spinal cord injury; siRNA, small interfering RNA.

expressed in the post-ischemic neurogenic niche.<sup>17,63</sup> In agreement with these reports, our findings show expression of FABP5 in putative neurogenic niches in the adult rat injured spinal cord. To support the claim that at least some FABP5<sup>+</sup> cells are neural progenitor cells (NPCs), we found colabeling of FABP5 with doublecortin (DCX), nestin, and the NG2 proteoglycan. NG2<sup>+</sup> progenitor cells are among the first cells to react to SCI. These self-renewing cells replenish oligodendrocyte populations within the intact stem cell niche. We have reported that DHA treatment increases the number of NPCs that express the NG2 proteoglycan in the lesion site at 7 dpi.<sup>13</sup> Whereas this effect may simply reflect the role of this FA to limit the expansion of injury, our findings substantiate the relevance of DHA metabolism in neuroplasticity and repair post-SCI. Studies have shown that NG2<sup>+</sup> progenitors born at 7 dpi can differentiate into oligodendrocytes that ensheath axons with myelin.<sup>69</sup> Therefore, it is a reasonable assumption that FABP5 may recapitulate its neurodevelopmental roles and promote survival, proliferation, and differentiation of NPCs post-SCI.

We have shown that induction of FABP5 during neurite outgrowth mobilizes FA substrates and is required for axon regeneration of retinal ganglion cells<sup>28</sup> and neurite formation in nerve-growth factor-differentiated PC12 cells.<sup>25,26,33</sup> These data are consistent with other reports implicating in the ability of PUFAs to promote neurite outgrowth.<sup>70-72</sup> FABP5 expression in structural biomarkers implicated in cytoskeletal and membrane turnover, including neurofilament<sup>+</sup> axons and GAP43<sup>+</sup> cells, suggests that

FABP5 may play roles in sites of active membrane synthesis, such as the DHA-rich growth cone.<sup>73</sup>

#### Targeting fatty acid transport to restore functional recovery after spinal cord injury

A remarkable finding of this study is that intrathecal administration of DHA, complexed to albumin or albumin alone (data not shown), induces significant improvements in motor function post-injury, validating the therapeutic efficacy of DHA and FA transport to ameliorate damage in animal models of neural injury.<sup>44,74,75</sup> Although the untargeted platforms used in this study did not provide neuroprotectin D1 (NPD1) levels, future targeted studies will be required to identify the metabolic underpinnings of DHA's protective effects. Animals treated with intrathecal DHA showed extensive movements of the hips, ankles, and knees while sweeping their hindlimbs at 7 dpi. Similar to our previous studies, we also observed a number of DHA-treated rats that showed occasional weight-supported stepping at 1 week post-injury.<sup>8,13</sup> Remarkably, administration of FABP5 siRNA abolished this beneficial effect in locomotor recovery post-SCI. We report a transient impairment in locomotor recovery in animals receiving FABP5 siRNA. This observation may reflect a role for FABP5 in modulation of early protective and reparative responses post-SCI.

In moving forward, it will be important to evaluate whether penetration, uptake, and bioactive signaling metabolites of DHA are altered after FABP5 siRNA administration. This remains a major challenge ahead because of possible cellular responses associated with lipid-mediated siRNA transfection and toxicity in neural cells. It is also important to unravel whether FABP5 interacts with other FAs implicated in repair after neurotrauma.<sup>4,15</sup>

#### Concluding Remarks

Our results establish that FABP5 is an important component in the subacute phase of SCI and may be required for important DHA-mediated repair processes associated with plasticity and functional recovery, such as neuroprotection, gliogenesis, neurogenesis, and neurite outgrowth. It is clear that a better understating of the transport and metabolism of n-3 PUFAs in the injured nervous system is needed before we can safely develop new treatments to facilitate endogenous repair mechanisms. For this reason, ongoing experiments in our lab are aimed at elucidating FABP-based strategies to accumulate n-3 PUFAs in the lesion milieu. Harnessing the beneficial responses to injury holds great potential to ameliorate neurotrauma outcomes. In this study, FABP5 emerges as a potential intracellular target for therapeutic intervention post-injury to the CNS.

#### Acknowledgments

The authors thank Dr. Manuel Montero, Dr. Odrick Rosas, Aranza Torrado, and Dr. Jose Santiago for help with animal care and surgical assistance. The authors also thank Lorena Salto for critical review and proofreading of the manuscript and for guidance and help with statistical analysis. The research reported in this publication was supported by grants P20MD006988 and 5R25GM060507. The content is solely the responsibility of the authors and does not necessarily represent the official views of the National Institutes of Health.

#### Author Disclosure Statement

No competing financial interests exist.

## References

- Hulsebosch, C.E. (2002). Recent advances in pathophysiology and treatment of spinal cord injury. *Adv. Physiol. Educ.* 26, 238–255.
- Hagg, T., and Oudega, M. (2006). Degenerative and spontaneous regenerative processes after spinal cord injury. *J. Neurotrauma* 23, 264–280.
- Yip, P.K., and Malaspina, A. (2012). Spinal cord trauma and the molecular point of no return. *Mol. Neurodegener.* 7, 6.
- Figueroa, J.D., and De Leon, M. (2014). Neurorestorative targets of dietary long-chain omega-3 fatty acids in neurological injury. *Mol. Neurobiol.* 50, 197–213.
- Anderson, D.K., and Hall, E.D. (1993). Pathophysiology of spinal cord trauma. *Ann. Emerg. Med.* 22, 987–992.
- Faden, A.I., Chan, P.H., and Longar, S. (1987). Alterations in lipid metabolism, Na<sup>+</sup>,K<sup>+</sup>-ATPase activity, and tissue water content of spinal cord following experimental traumatic injury. *J. Neurochem.* 48, 1809–1816.
- Fujieda, Y., Ueno, S., Ogino, R., Kuroda, M., Jönsson, T.J., Guo, L., Bamba, T., and Fukusaki, E. (2012). Metabolite profiles correlate closely with neurobehavioral function in experimental spinal cord injury in rats. *PLoS ONE* 7, e43152.
- Figueroa, J.D., Cordero, K., Ilán, M.S., and De Leon, M. (2013). Dietary omega-3 polyunsaturated fatty acids improve the neurolipidome and restore the DHA status while promoting functional recovery after experimental spinal cord injury. *J. Neurotrauma* 30, 853–868.
- Huang, W.L., King, V.R., Curran, O.E., Dyllal, S.C., Ward, R.E., Lal, N., Priestley, J.V., and Michael-Titus, A.T. (2007). A combination of intravenous and dietary docosahexaenoic acid significantly improves outcome after spinal cord injury. *Brain* 130, 3004–3019.
- King, V.R., Huang, W.L., Dyllal, S.C., Curran, O.E., Priestley, J.V., and Michael-Titus, A.T. (2006). Omega-3 fatty acids improve recovery, whereas omega-6 fatty acids worsen outcome, after spinal cord injury in the adult rat. *J. Neurosci.* 26, 4672–4680.
- Lang-Lazdunski, L., Blondeau, N., Jarretou, G., Lazdunski, M., and Heurteaux, C. (2003). Linolenic acid prevents neuronal cell death and paraplegia after transient spinal cord ischemia in rats. *J. Vasc. Surg.* 38, 564–575.
- Ward, R.E., Huang, W., Curran, O.E., Priestley, J.V., and Michael-Titus, A.T. (2010). Docosahexaenoic acid prevents white matter damage after spinal cord injury. *J. Neurotrauma* 27, 1769–1780.
- Figueroa, J.D., Cordero, K., Baldeosingh, K., Torrado, A.I., Walker, R.L., Miranda, J.D., and Leon, M.D. (2012). Docosahexaenoic acid pretreatment confers protection and functional improvements after acute spinal cord injury in adult rats. *J. Neurotrauma* 29, 551–566.
- Murphy, E.J., Behrmann, D., Bates, C.M., and Horrocks, L.A. (1994). Lipid alterations following impact spinal cord injury in the rat. *Mol. Chem. Neuropathol.* 23, 13–26.
- Figueroa, J.D., Cordero, K., Serrano-Illan, M., Almeyda, A., Baldeosingh, K., Almaguel, F.G., and De Leon, M. (2013). Metabolomics uncovers dietary omega-3 fatty acid-derived metabolites implicated in anti-nociceptive responses after experimental spinal cord injury. *Neuroscience* 255, 1–18.
- Lim, S.-N., Huang, W., Hall, J.C.E., Michael-Titus, A.T., and Priestley, J.V. (2013). Improved outcome after spinal cord compression injury in mice treated with docosahexaenoic acid. *Exp. Neurol.* 239, 13–27.
- Matsumata, M., Sakayori, N., Maekawa, M., Owada, Y., Yoshikawa, T., and Osumi, N. (2012). The effects of Fabp7 and Fabp5 on postnatal hippocampal neurogenesis in the mouse. *Stem Cells* 30, 1532–1543.
- Shioda, N., Yamamoto, Y., Watanabe, M., Binas, B., Owada, Y., and Fukunaga, K. (2010). Heart-type fatty acid binding protein regulates dopamine D2 receptor function in mouse brain. *J. Neurosci.* 30, 3146–3155.
- Yu, S., Levi, L., Casadesus, G., Kunos, G., and Noy, N. (2014). Fatty acid-binding protein 5 (FABP5) regulates cognitive function both by decreasing anandamide levels and by activating the nuclear receptor peroxisome proliferator-activated receptor  $\beta/\delta$  (PPAR $\beta/\delta$ ) in the brain. *J. Biol. Chem.* 289, 12748–12758.
- Gerstner, J.R., Vanderheyden, W.M., LaVaute, T., Westmark, C.J., Rouhana, L., Pack, A.I., Wickens, M., and Landry, C.F. (2012). Time of day regulates subcellular trafficking, tripartite synaptic localization, and polyadenylation of the astrocytic Fabp7 mRNA. *J. Neurosci.* 32, 1383–1394.
- Hanhoff, T., Lücke, C., and Spener, F. (2002). Insights into binding of fatty acids by fatty acid binding proteins. *Mol. Cell. Biochem.* 239, 45–54.
- Xu, L.Z., Sánchez, R., Sali, A., and Heintz, N. (1996). Ligand specificity of brain lipid-binding protein. *J. Biol. Chem.* 271, 24711–24719.
- Balendiran, G.K., Schnütgen, F., Scapin, G., Borchers, T., Xhong, N., Lim, K., Godbout, R., Spener, F., and Sacchettini, J.C. (2000). Crystal structure and thermodynamic analysis of human brain fatty acid-binding protein. *J. Biol. Chem.* 275, 27045–27054.
- Kane, C.D., Coe, N.R., Vanlandingham, B., Krieg, P., and Bernlohr, D.A. (1996). Expression, purification, and ligand-binding analysis of recombinant keratinocyte lipid-binding protein (MAL-1), an intracellular lipid-binding found overexpressed in neoplastic skin cells. *Biochemistry* 35, 2894–2900.
- Liu, J.-W., Almaguel, F.G., Bu, L., De Leon, D.D., and De Leon, M. (2008). Expression of E-FABP in PC12 cells increases neurite extension during differentiation: involvement of n-3 and n-6 fatty acids. *J. Neurochem.* 106, 2015–2029.
- Liu, Y., Molina, C.A., Welcher, A.A., Longo, L.D., and De Leon, M. (1997). Expression of DA11, a neuronal-injury-induced fatty acid binding protein, coincides with axon growth and neuronal differentiation during central nervous system development. *J. Neurosci. Res.* 48, 551–562.
- Liu, Y., Longo, L.D., and De Leon, M. (2000). In situ and immunocytochemical localization of E-FABP mRNA and protein during neuronal migration and differentiation in the rat brain. *Brian Res.* 852, 16–27.
- Allen, G.W., Liu, J., Kirby, M.A., and De Leon, M. (2001). Induction and axonal localization of epithelial/epidermal fatty acid-binding protein in retinal ganglion cells are associated with axon development and regeneration. *J. Neurosci. Res.* 66, 396–405.
- Boneva, N.B., Mori, Y., Kaplamadzhiev, D.B., Kikuchi, H., Zhu, H., Kikuchi, M., Tonchev, A.B., and Yamashima, T. (2010). Differential expression of FABP 3, 5, 7 in infantile and adult monkey cerebellum. *Neurosci. Res.* 68, 94–102.
- Owada, Y., Yoshimoto, T., and Kondo, H. (1996). Increased expression of the mRNA for brain- and skin-type but not heart-type fatty acid binding proteins following kainic acid systemic administration in the hippocampal glia of adult rats. *Brain Res. Mol. Brain Res.* 42, 156–160.
- De Leon, M., Welcher, A.A., Nahin, R.H., Liu, Y., Ruda, M.A., Shooter, E.M., and Molina, C.A. (1996). Fatty acid binding protein is induced in neurons of the dorsal root ganglia after peripheral nerve injury. *J. Neurosci. Res.* 44, 283–292.
- Ma, D., Zhang, M., Mori, Y., Yao, C., Larsen, C.P., Yamashima, T., and Zhou, L. (2010). Cellular localization of epidermal-type and brain-type fatty acid-binding proteins in adult hippocampus and their response to cerebral ischemia. *Hippocampus* 20, 811–819.
- Allen, G.W., Liu, J.W., and De León, M. (2000). Depletion of a fatty acid-binding protein impairs neurite outgrowth in PC12 cells. *Brain Res. Mol. Brain Res.* 76, 315–324.
- Liu, J.-W., Montero, M., Bu, L., and De Leon, M. (2015). Epidermal fatty acid-binding protein protects nerve growth factor-differentiated PC12 cells from lipotoxic injury. *J. Neurochem.* 132, 85–98.
- Gruner, J.A. (1992). A monitored contusion model of spinal cord injury in the rat. *J. Neurotrauma* 9, 123–126; discussion, 126–128.
- Kumar, K.K., Goodwin, C.R., Uhouse, M.A., Bornhorst, J., Schwerdtle, T., Aschner, M., McLean, J.A., and Bowman, A.B. (2015). Untargeted metabolic profiling identifies interactions between Huntington's disease and neuronal manganese status. *Metallomics* 7, 363–370.
- McFadden, J.W., Aja, S., Li, Q., Bandaru, V.V.R., Kim, E.-K., Haughey, N.J., Kuhajda, F.P., and Ronnett, G.V. (2014). Increasing fatty acid oxidation remodels the hypothalamic neurometabolome to mitigate stress and inflammation. *PLoS ONE* 9, e115642.
- Blankman, J.L., Long, J.Z., Trauger, S.A., Siuzdak, G., and Cravatt, B.F. (2013). ABHD12 controls brain lysophosphatidylserine pathways that are deregulated in a murine model of the neurodegenerative disease PHARC. *Proc. Natl. Acad. Sci. U. S. A.* 110, 1500–1505.
- Blasco, H., Corcia, P., Pradat, P.-F., Bocca, C., Gordon, P.H., Veyrat-Durebex, C., Mavel, S., Nadal-Desbarats, L., Moreau, C., Devos, D., Andres, C.R., and Emond, P. (2013). Metabolomics in cerebrospinal fluid of patients with amyotrophic lateral sclerosis: an untargeted

- approach via high-resolution mass spectrometry. *J. Proteome Res.* 12, 3746–3754.
40. Dehaven, C.D., Evans, A.M., Dai, H., and Lawton, K.A. (2010). Organization of GC/MS and LC/MS metabolomics data into chemical libraries. *J. Cheminform.* 2, 9.
  41. Figueroa, J.D., Benton, R.L., Velazquez, I., Torrado, A.I., Ortiz, C.M., Hernandez, C.M., Diaz, J.J., Magnuson, D.S., Whittemore, S.R., and Miranda, J.D. (2006). Inhibition of EphA7 up-regulation after spinal cord injury reduces apoptosis and promotes locomotor recovery. *J. Neurosci. Res.* 84, 1438–1451.
  42. Cruz-Orengo, L., Figueroa, J.D., Torrado, A., Puig, A., Whittemore, S.R., and Miranda, J.D. (2007). Reduction of EphA4 receptor expression after spinal cord injury does not induce axonal regeneration or return of tcmMEEP response. *Neurosci. Lett.* 418, 49–54.
  43. Basso, D.M., Beattie, M.S., and Bresnahan, J.C. (1995). A sensitive and reliable locomotor rating scale for open field testing in rats. *J. Neurotrauma* 12, 1–21.
  44. Belayev, L., Marcheselli, V.L., Khoutorova, L., Rodriguez de Turco, E.B., Busto, R., Ginsberg, M.D., and Bazan, N.G. (2005). Docosahexaenoic acid complexed to albumin elicits high-grade ischemic neuroprotection. *Stroke* 36, 118–123.
  45. Luo, M.-C., Zhang, D.-Q., Ma, S.-W., Huang, Y.-Y., Shuster, S.J., Poreca, F., and Lai, J. (2005). An efficient intrathecal delivery of small interfering RNA to the spinal cord and peripheral neurons. *Mol. Pain* 1, 29–29.
  46. Cruz-Orengo, L., Figueroa, J.D., Velazquez, I., Torrado, A., Ortiz, C., Hernández, C., Puig, A., Segarra, A.C., Whittemore, S.R., and Miranda, J.D. (2006). Blocking EphA4 upregulation after spinal cord injury results in enhanced chronic pain. *Exp. Neurol.* 202, 421–433.
  47. Xia, J., Sinelnikov, I.V., Han, B., and Wishart, D.S. (2015). *MetaboAnalyst 3.0*—making metabolomics more meaningful. *Nucleic Acids Res.* 43, W251–W257.
  48. Bailes, J.E., and Mills, J.D. (2010). Docosahexaenoic acid reduces traumatic axonal injury in a rodent head injury model. *J. Neurotrauma* 27, 1617–1624.
  49. Wu, A., Ying, Z., and Gómez-Pinilla, F. (2004). Dietary omega-3 fatty acids normalize BDNF levels, reduce oxidative damage, and counteract learning disability after traumatic brain injury in rats. *J. Neurotrauma* 21, 1457–1467.
  50. Satkunendrarajah, K., and Fehlings, M.G. (2013). Do omega-3 polyunsaturated fatty acids ameliorate spinal cord injury?: Commentary on: Lim et al., Improved outcome after spinal cord compression injury in mice treated with docosahexaenoic acid. *Exp. Neurol. Jan; 239:13–27. Exp. Neurol.* 249C, 104–110.
  51. Haunerland, N.H., and Spener, F. (2004). Fatty acid-binding proteins—insights from genetic manipulations. *Prog. Lipid Res.* 43, 328–349.
  52. Shimamoto, C., Ohnishi, T., Maekawa, M., Watanabe, A., Ohba, H., Arai, R., Iwayama, Y., Hisano, Y., Toyota, T., Toyoshima, M., Suzuki, K., Shirayama, Y., Nakamura, K., Mori, N., Owada, Y., Kobayashi, T., and Yoshikawa, T. (2014). Functional characterization of FABP3, 5 and 7 gene variants identified in schizophrenia and autism spectrum disorder and mouse behavioral studies. *Hum. Mol. Genet.* 23, 6495–6511.
  53. Schnell, A., Chappuis, S., Schmutz, I., Brai, E., Ripperger, J.A., Schaad, O., Welzl, H., Descombes, P., Alberi, L., and Albrecht, U. (2014). The nuclear receptor REV-ERB $\alpha$  regulates Fabp7 and modulates adult hippocampal neurogenesis. *PLoS ONE* 9, e99883.
  54. Kaczocha, M., Rebecchi, M.J., Ralph, B.P., Teng, Y.-H.G., Berger, W.T., Galbavy, W., Elmes, M.W., Glaser, S.T., Wang, L., Rizzo, R.C., Deutsch, D.G., and Ojima, I. (2014). Inhibition of fatty acid binding proteins elevates brain anandamide levels and produces analgesia. *PLoS ONE* 9, e94200.
  55. Rao, E., Singh, P., Li, Y., Zhang, Y., Chi, Y.-I., Suttles, J., and Li, B. (2015). Targeting epidermal fatty acid binding protein for treatment of experimental autoimmune encephalomyelitis. *BMC Immunol.* 16, 28.
  56. Murphy, E.J., Owada, Y., Kitanaka, N., Kondo, H., and Glatz, J.F.C. (2005). Brain arachidonic acid incorporation is decreased in heart fatty acid binding protein gene-ablated mice. *Biochemistry* 44, 6350–6360.
  57. Murphy, E.J., Barceló-Coblijn, G., Binas, B., and Glatz, J.F.C. (2004). Heart fatty acid uptake is decreased in heart fatty acid-binding protein gene-ablated mice. *J. Biol. Chem.* 279, 34481–34488.
  58. Desai, A., Kevala, K., and Kim, H.-Y. (2014). Depletion of brain docosahexaenoic acid impairs recovery from traumatic brain injury. *PLoS ONE* 9, e86472.
  59. Odani, S., Nakamura, J., Sato, T., and Fujii, H. (2001). Identification of a rat 30-kDa protein recognized by the antibodies to a recombinant rat cutaneous fatty acid-binding protein as a 14-3-3 protein. *J. Biochem.* 129, 213–219.
  60. Bennaars-Eiden, A., Higgins, L., Hertz, A.V., Kappahn, R.J., Ferrington, D.A., and Bernlohr, D.A. (2002). Covalent modification of epithelial fatty acid-binding protein by 4-hydroxynonenal in vitro and in vivo. Evidence for a role in antioxidant biology. *J. Biol. Chem.* 277, 50693–50702.
  61. Pelsers, M.M., and Glatz, J.F.C. (2005). Detection of brain injury by fatty acid-binding proteins. *Clin. Chem. Lab. Med.* 43, 802–809.
  62. Saino-Saito, S., Nourani, R.M., Iwasa, H., Kondo, H., and Owada, Y. (2009). Discrete localization of various fatty-acid-binding proteins in various cell populations of mouse retina. *Cell Tissue Res.* 338, 191–201.
  63. Boneva, N.B., Kaplamadzhiev, D.B., Sahara, S., Kikuchi, H., Pyko, I.V., Kikuchi, M., Tonchev, A.B., and Yamashima, T. (2011). Expression of fatty acid-binding proteins in adult hippocampal neurogenic niche of posts ischemic monkeys. *Hippocampus* 21, 162–171.
  64. Owada, Y. (2008). Fatty acid binding protein: localization and functional significance in the brain. *Tohoku J. Exp. Med.* 214, 213–220.
  65. White, R.E., McTigue, D.M., and Jakeman, L.B. (2010). Regional heterogeneity in astrocyte responses following contusive spinal cord injury in mice. *J. Comp. Neurol.* 518, 1370–1390.
  66. Shariif, K., Morihiro, Y., Maekawa, M., Yasumoto, Y., Hoshi, H., Adachi, Y., Sawada, T., Tokuda, N., Kondo, H., Yoshikawa, T., Suzuki, M., and Owada, Y. (2011). FABP7 expression in normal and stab-injured brain cortex and its role in astrocyte proliferation. *Histochem. Cell Biol.* 136, 501–513.
  67. Moore, S.A. (2001). Polyunsaturated fatty acid synthesis and release by brain-derived cells in vitro. *J. Mol. Neurosci.* 16, 195–200; discussion, 215–221.
  68. Williard, D.E., Harmon, S.D., Kaduce, T.L., Preuss, M., Moore, S.A., Robbins, M.E., and Spector, A.A. (2001). Docosahexaenoic acid synthesis from n-3 polyunsaturated fatty acids in differentiated rat brain astrocytes. *J. Lipid Res.* 42, 1368–1376.
  69. Sellers, D.L., Maris, D.O., and Horner, P.J. (2009). Postinjury niches induce temporal shifts in progenitor fates to direct lesion repair after spinal cord injury. *J. Neurosci.* 29, 6722–6733.
  70. Calderon, F., and Kim, H.-Y. (2004). Docosahexaenoic acid promotes neurite growth in hippocampal neurons. *J. Neurochem.* 90, 979–988.
  71. Robson, L.G., Dyall, S., Sidloff, D., and Michael-Titus, A.T. (2010). Omega-3 polyunsaturated fatty acids increase the neurite outgrowth of rat sensory neurones throughout development and in aged animals. *Neurobiol. Aging* 31, 678–687.
  72. Nakato, M., Matsuo, M., Kono, N., Arita, M., Arai, H., Ogawa, J., Kioka, N., and Ueda, K. (2015). Neurite outgrowth stimulation by n3 and n6 polyunsaturated fatty acids of phospholipids in apolipoprotein E containing lipoproteins secreted from glial cells. *J. Lipid Res.* 56, 1880–1890.
  73. Auestad, N., and Innis, S.M. (2000). Dietary n-3 fatty acid restriction during gestation in rats: neuronal cell body and growth-cone fatty acids. *Am. J. Clin. Nutr.* 71, 1 Suppl., 312S–314S.
  74. Berman, D.R., Liu, Y.Q., Barks, J., and Mozurkewich, E. (2010). Docosahexaenoic acid confers neuroprotection in a rat model of perinatal hypoxia-ischemia potentiated by *Escherichia coli* lipopolysaccharide-induced systemic inflammation. *Am. J. Obstet. Gynecol.* 202, 469.e1–6.
  75. Berman, D.R., Mozurkewich, E., Liu, Y., and Barks, J. (2009). Docosahexaenoic acid pretreatment confers neuroprotection in a rat model of perinatal cerebral hypoxia-ischemia. *Am. J. Obstet. Gynecol.* 200, 305.e1–6.

Address correspondence to:

Marino De Leon, PhD  
 Center for Health Disparities and Molecular Medicine  
 School of Medicine  
 Loma Linda University  
 11085 Campus Street  
 Loma Linda, CA 92350

E-mail: madeleon@llu.edu